Prediction of Lab Scale Cross-Flow Tidal Turbine Performance Using Unsteady RANS

R. M. Stringer[#1], J.Zang[#2], A.J.Hillis[*3]

[#]*Department of Architecture & Civil Engineering, University of Bath*
Bath, BA2 7AY, UK

[1]r.m.stringer@bath.ac.uk

[2]j.zang@bath.ac.uk

[*]*Department of Mechanical Engineering, University of Bath*
Bath, BA2 7AY, UK

[3]a.j.hillis@bath.ac.uk

***Abstract*— A cross-flow tidal turbine developed and experimentally tested by the University of Oxford has been numerically modelled using the commercial computational fluid dynamics solver ANSYS CFX 14.0. The issue of scaling is specifically addressed with emphasis on establishing performance reduction due to low blade chord Reynolds number. Building upon single blade validation, a fully transient numerical tank and turbine is defined and tested. Despite 2D simplification, results give high qualitative agreement with experimental values providing an insight into flow phenomenon through the turbine. The model is finally used to explore a number of flow scenarios, scale and blockage effects.**

***Keywords*— Tidal Turbine, Cross-Flow, CFD, Reynolds number**

Nomenclature
D = Drag
L = Lift
r = radius
Re = Reynolds number
U = Flow velocity
θ = Blade position angle
μ = Kinematic viscosity of water
ρ = Density of water
ω = Angular velocity

I. Introduction

The engineering design process for a new tidal turbine inevitably leads to the construction of a prototype for laboratory and small scale testing. A consequence of the reduced size is a reduction in lift and drag performance due to Reynolds number scaling effects. This is further complicated by an increase in performance due to channel blockage. To understand these processes and quantify their impact, a robust numerical model of a prototype tidal turbine is developed. The study utilises an existing set of data acquired by a cross-flow turbine designed and experimentally tested by the University of Oxford. Specifically, the device investigated is a 3-bladed fixed pitch transverse turbine, built to a 1/20th scale, see [1] for details. The numerical reproduction of the experiment and subsequent results are outlined in this paper.

The cross-flow turbine has received growing interest from both academia and industry, with leading examples including the University of Oxford 'THAWT' device (now Kepler Energy) [2], Italian developer Ponti di Archimede Internantional's 'Kobold' turbine [3] and the "Gorlov" helical design [4] The alternative rotor design offers a number of prospective advantages over the conventional axial configuration; primarily form factor, scalability, survivability and channel blockage.

The concept of operation of the cross-flow design was conceived by Darrieus in his 1931 patent for a wind turbine [5]. The principle is directly applicable to today's tidal designs, a schematic of which is depicted in Fig. 1. The diagram shows a three blade turbine turning anticlockwise about axis Z. Resolving rotation velocity (U_{tan}) and free stream velocity (U^{∞}), an effective velocity (U_{eff}) is obtained, along with a corresponding effective angle of attack (α). The resulting lift (L) generated from the perceived velocity and flow direction provides the driving torque of the system. The efficiency of a fixed pitch device in uniform flow is primarily a function of Tip Speed Ratio (TSR) or $\lambda = U_{tan}/U^{\infty}$, too slow and excessive stall occurs, too fast and angle of attack (α) becomes insufficient to induce useful lift.

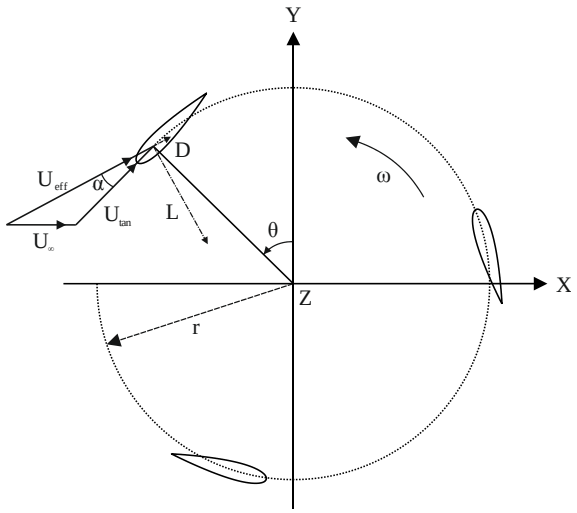

Fig. 1. Schematic of cross-flow turbine identifying functional parameters

II. Uncertainties of Scale

The hydrodynamic performance of tidal turbines has been commonly related to a number of parameters, including Froude number, Reynolds number and blockage ratio amongst others. The Froude number, a non-dimensional ratio of the inertial and gravitational energy, provides an indication of the available energy to the turbine. Existing research shows that the relationship of Froude number to turbine performance is still uncertain due to variables including free-surface proximity and distinction of the value from the effects of blockage [6]. As part of a laboratory scale experimental study by McAdam [7], a correlation between an increasing Froude number and an increasing turbine performance was identified. However, Reynolds number is also increased, with an unknown contribution. The research here focusses on addressing this issue in relation to lab scale testing. The Reynolds number, given below, relates inertial and viscous forces on a body of a given size.

$$Re = \frac{\rho U D}{\mu}$$

A full scale turbine of the Oxford design would potentially have a blade chord Reynolds number greater than 10^6, however, at lab scale this is reduced to ≈ 50,000 – 90,000.

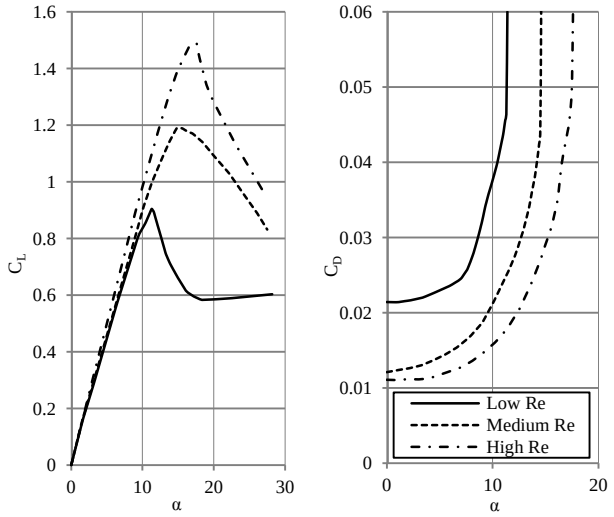

Fig. 2. Lift (Left) and Drag (Right) coefficients at a range of angles of attack for Reynolds numbers; Low = 81,000, Medium = 654,000, High = 3,150,000 [8, 9]

Using aerodynamic data for a range of Reynolds numbers, Fig. 2 displays curves for coefficient of lift (C_L) and drag (C_D) for a NACA 0018 profile blade. The data shows a distinct reduction in stall angle, peak lift, as well as an increase in drag at all angles of attack with decreasing Reynolds number. The lower Reynolds value of 81,000 is equivalent to that experienced by the Oxford turbine, highlighting the expected loss in performance. Additional phenomena at low Reynolds numbers are also present including formation of separation bubbles as well as Kelvin-Helmholts and Tollmien-Schlichting instabilities.

III. Numerical Testing

The development of the numerical model is taken in two stages; first an individual blade is refined and validated, followed by a full turbine model of the experimental turbine.

A. Individual Blade

A single NACA 0018 blade was numerically simulated at angles of attack from 0 to 25 degrees. The commercial solver ANSYS CFX 14.0 was used for all simulations.

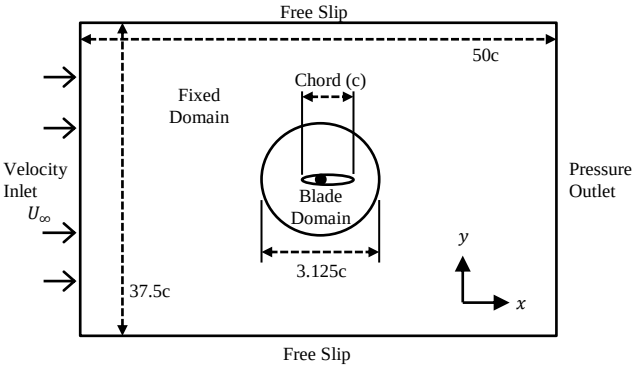

Fig. 3. Diagram of single blade testing numerical domain

The general characteristics of the numerical setup are shown in Fig. 3. The blade is located in a cylindrical central domain which allows for angle of attack to be altered without remeshing, as well as providing a limit for the near blade mesh refinement. This is surrounded by a large 'Fixed Domain' sufficiently sized to make blockage negligible. A GGI interface connects the domains, with outer boundaries constrained as indicated in Fig. 3.

As the modelling focussed on 2D, a RANS approach was taken using the k-ω SST model. Testing was conducted at a blade chord Reynolds number of 81,000, which is within the region of the experimental model, plus allowed for direct comparison with existing data for validation.

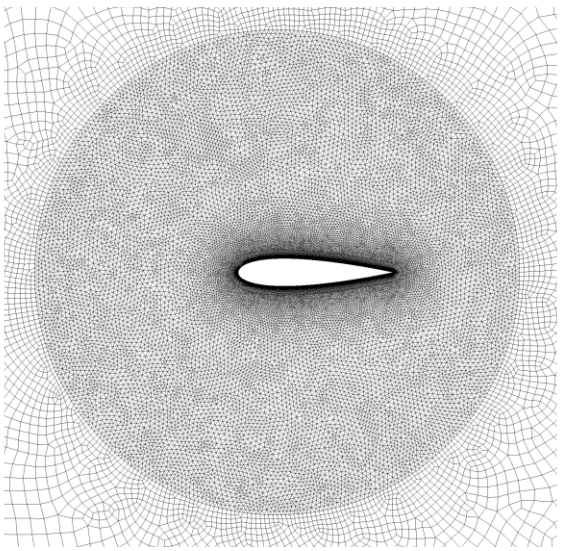

Fig. 4. Close up view of the 'Blade Domain' final mesh

With separation being a common issue for low Reynolds number hydrofoil profiles, appropriate mesh refinement was found to be essential. A study was conducted for numerous meshing parameters, although specific attention was given to blade surface spacing and y^+ (or yPlus) conformity. Fig. 4 shows the final result of the process, consisting of structured hexahedral layers at the blades surface, unstructed highly refined wedges in the near field, and a hexahedral outer domain (appearing disordered close to the interface).

The results indicated that y^+ was the most critical factor in achieving correlation with experimental values. For this reason, results are plotted for coefficients of lift and drag in Figs. 5-6 for a number of maximum y^+ value conditions.

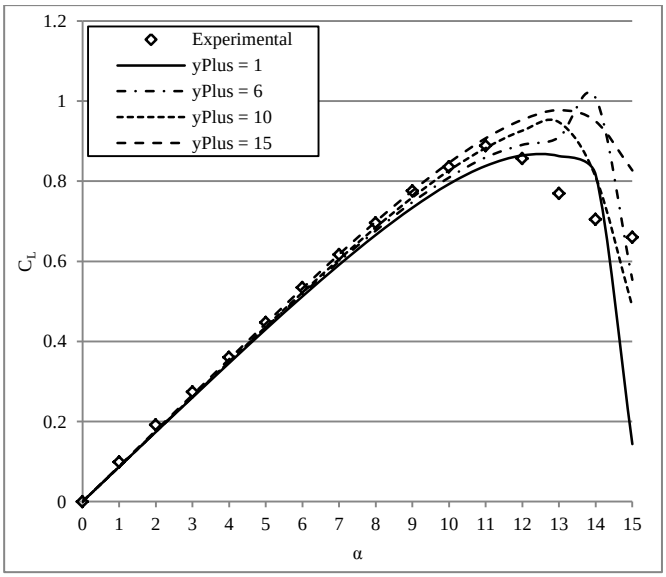

Fig. 5. Graph of lift coefficient vs. angle of attack; experimental and numerical results for a number of y^+ mesh qualities. Experimental source [8]

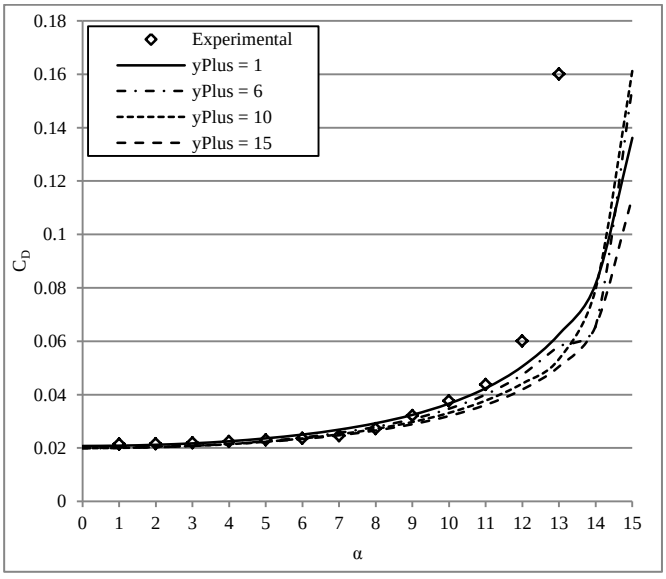

Fig. 6. Graph of drag coefficient vs. angle of attack; experimental and numerical results for a number of y^+ mesh qualities. Experimental source [8]

The data used in Figs. 5-6 is corrected by the original authors to approximate at 'infinite aspect ratio' blade, equivalent to 2D. It can be concluded that a lower y^+ leads to an improved agreement in drag, while lift is slightly under predicted. However, higher values of y^+ increase the peak lift and reduce drag to unrealistic levels, therefore a compromise of a maximum y^+=10 is selected for full turbine analysis. At higher angles of attack (not shown), instability of the solution was experienced due to large regions of unsteady separation. This is an expected limitation of RANS, and is avoided by concentrating on TSRs with resultant peak angles of attack below 15 degrees.

B. Full Turbine Simulation

The experimental turbine data was collected from a prototype Transverse Horizontal Axis Water Turbine (THAWT) developed by the University of Oxford. The turbine consists of three NACA 0018 blades circumferentially wrapped about their circular flight patch fastened between solid aluminium plates. The turbine is mounted transverse to the flow such that the axis is horizontal and flow passes from left to right as depicted in Fig. 1. Table I provides a summary of experimental environment and turbine sizing.

TABLE I
EXPERIMENTAL ATTRIBUTES

Parameter	Value
Flume width (m)	1.8
Width at constriction (m)	1.61
Flow depth (m)	1.0
Height of rotor axis above flume base (m)	0.425
Rotor diameter (m)	0.50
Parallel cross flow span of blades (m)	1.528
Rotor solidity	0.125
Parallel blade chord (mm)	65.45

Converting the experimental case into a 2D computational model caused two key difficulties. Firstly the flume employed produced a high velocity shear in the flow, and secondly the turbine was placed in a constriction due to space requirements for mechanical connections at either side of the turbine. These behaviours were accounted for in the computational model by using an interpolated velocity scheme at the inlet and by increasing the overall velocity by the ratio of the narrows; 1.8/1.61 (shown in Table I).

The full model consists of three blade domains, as developed in the individual blade phase, a rotating domain and a fixed domain, as shown in Fig. 7.

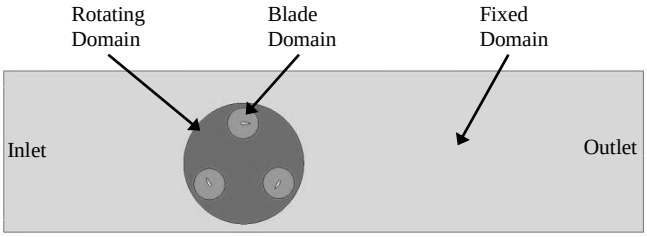

Fig. 7. Layout of the full turbine numerical tank

The geometry and boundary conditions of the experimental tank were matched, apart from the free surface (top side of Fig. 7) which was set to a 'free slip' condition. Far field Mesh and timestep sensitivity studies were conducted to achieve maximum correlation with experimental results.

The data selected for comparison includes the blade loading, collected by means of a load cell of the experimental blade, and the power output of the turbine. TSRs of 2, 3, and 4 were computed with a quasi steady state being reached for all transient values.

Results are shown for TSRs of 2, 3 and 4 in Figs. 8, 9 and 10 respectively. Beginning with the slow spinning turbine, at a TSR of 2, large discrepancies are visible in the 180-360 degree region. Referring to Fig. 1, at rotation angles (θ) below 180 degrees the blades are upstream, and above 180 degrees they are downstream. A combination of being in the wake of the upstream blades, and the slow TSR have caused heavy stall of the downstream blades. As expected the RANS method is unable to accurately predict forces under such conditions.

At a TSR of 3, Fig. 9 shows a much improved correlation with the experimental readings. The positives include a qualitatively high match, with almost all of the peaks and troughs captured by the numerical model. Quantitatively the zero degree value and the downstream values are below expected. Causes include possible free surface effects for values close to zero degrees, and the inability of the 2D model to fully compensate for the constricting and diverging flume side walls identified in Table I.

Increasing the speed of the turbine to a TSR of 4, Fig. 10 shows similar attributes to those in Fig. 9. The upstream quantitative values are particularly well matched with the extreme loading predicted within 5% of the experimental value. Downstream the result appears to diverge significantly from experimental values. This suggests that more energy is available to the turbine than the numerical solution is predicting. Possible reasons include a higher turbulence and hence faster wake recovery, as well as an increasing impact of the diverging flume walls.

With the most significant match falling at a TSR of 3, the model was employed to explore a number of alternative flow scenarios including:

- A full scale turbine (10x larger)
- Uniform inflow (blockage 0.5)
- Uniform inflow (blockage 0.1)
- 1/5th Power law inlet profile

For each case the power coefficient (C_P) is calculated using the turbine output power (P) divided by the kinetic energy available across the rotor area (A), see equation below:

$$C_P = \frac{P}{\frac{1}{2}\rho U^3 A}$$

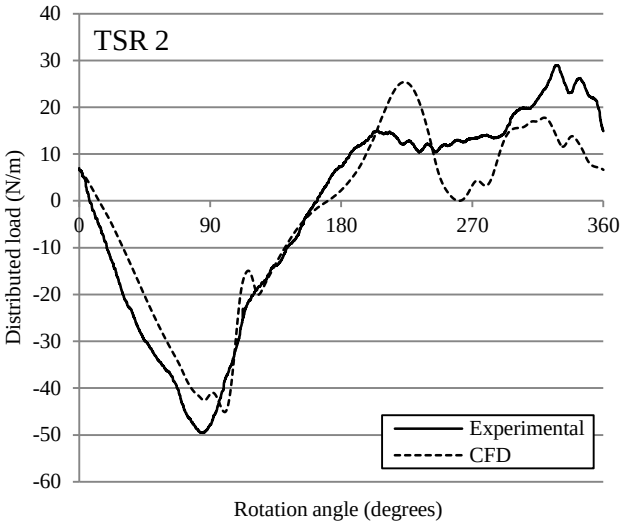

Fig. 8. Graph of distributed load vs. rotation angle for a TSR of 2

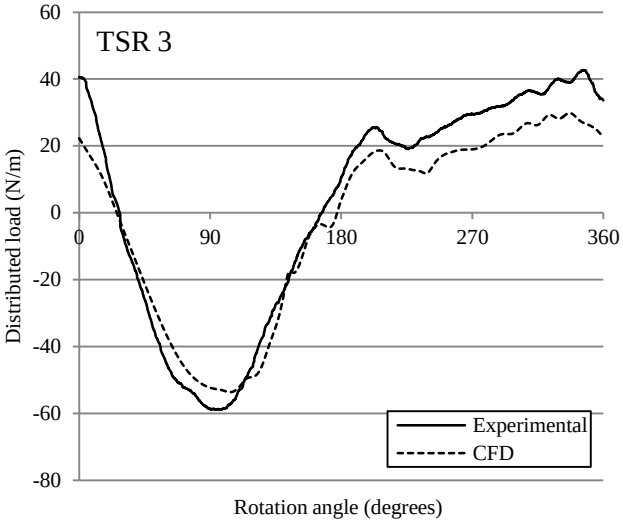

Fig. 9. Graph of distributed load vs. rotation angle for a TSR of 3

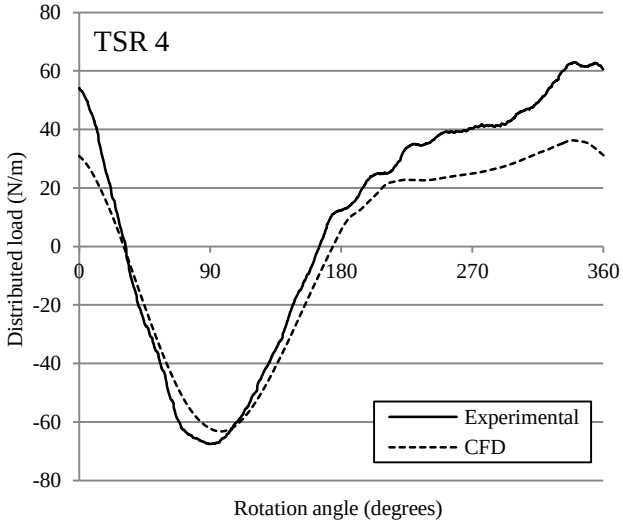

Fig. 10. Graph of distributed load vs. rotation angle for a TSR of 4

TABLE II
TURBINE POWER COEFFICIENTS

Scenario	C_P
Lab Scale (Experiment)	0.47
Lab Scale (Numerical)	0.47
Full Scale (x10)	0.95
Uniform Flow (Blockage 0.5)	0.58
Uniform Flow (Blockage 0.1)	0.27
$1/5^{th}$ Power Law	0.55

With the exception of the single experimental value, Table II shows numerically predicted power outputs for a number of turbine environments. The first two rows compare the original experimental data with the numerical prediction. The result is a match due to a marginally smaller torque from the simulation being offset by a marginally higher rotational speed, an alteration made to account for the flume constriction.

The large scale result shows an increase of over double the power coefficient. Referring to Figs. 11 and 12, the source of the additional power can be identified. Fig. 11 shows a vorticity plot of the lab scale result where extensive dynamic stall can be seen as the blades travel downstream. Conversely, the full scale turbine result in Fig. 12 shows full attachment throughout the 360 degree rotation. With velocities remaining equal in both cases, the Reynolds number can be identified as a defining factor in flow attachment and hence power output.

Comparing the two blockage cases, both computed at lab scale, the effect of reducing blockage is significant, with the resulting turbine providing less than half the power. Further simulations are planned to explore the relationship further.

Finally the $1/5^{th}$ power law, considered to be a realistic velocity profile for tidal turbine sites, provides around 5% less than the ideal uniform flow. The limitations of testing in a flume are highlighted by the original lab scale velocity profile giving the lowest C_P when compared to cases also sited in the flume.

IV. CONCLUSIONS

A 2D numerical model of a cross-flow lab scale turbine has been developed and validated against experimental data. High qualitative agreement has been achieved, particularly for mid-range TSR values most suited to the unsteady RANS methodology. The 2D approximation is more that capable of providing an insight into the flow structure through a cross-flow tidal turbine and is being used to explore advantages and disadvantages regarding siting possibilities and turbine configuration. One of the key purposes of the study was to identify the importance of Reynolds number when scaling a device for lab testing. The result is that a clear loss in performance is to be expected, not only due to lower lift and drag performance, but also due to the resultant dynamic vortex shedding. Based on these findings it is advised that lab scale tests should aim to achieve the highest Reynolds numbers possible.

ACKNOWLEDGMENT

For supplying the experimental data for this study I would like to thank the University of Oxford and Kepler Energy Ltd.

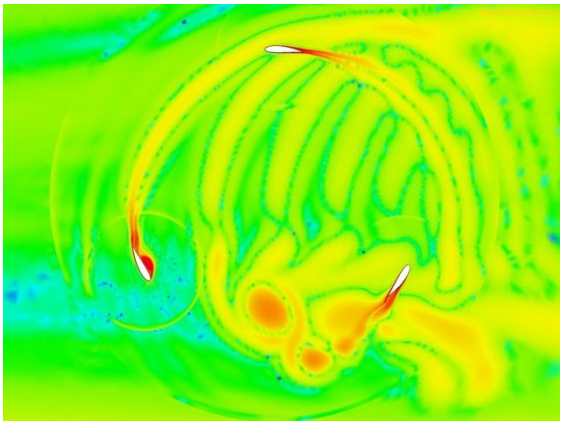

Fig. 11. Vorticity plot of the numerical result at lab scale

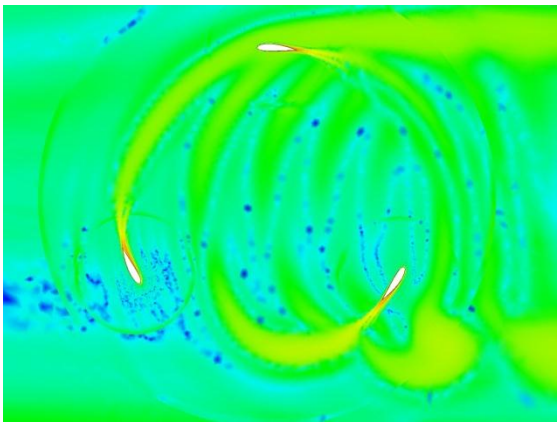

Fig. 12. Vorticity plot of the numerical result at full scale

REFERENCES

[1] McAdam, R.A., G.T. Houlsby, and M.L.G. Oldfield, Experimental measurements of the hydrodynamic performance and structural loading of the Transverse Horizontal Axis Water Turbine: Part 1. Renewable Energy, 2013. 59(0): p. 105-114.

[2] University of Oxford. Tidal Energy Research Group. Available from: http://www.eng.ox.ac.uk/tidal/research/thawt.

[3] Calcagno, G., et al., Experimental and numerical investigation of an innovative technology for marine current exploitation: the Kobold turbine. Proceedings of the Sixteenth (2006) International Offshore and Polar Engineering Conference, Vol 1, 2006: p. 323-330.

[4] Gorlov, A.M., The helical turbine: A new idea for low-head hydropower. Hydro Review, 1995(14): p. 44--50.

[5] Darrieus, G.J.M., Turbine having its rotating shaft transverse to the flow of the current, U.S.P. Office, Editor. 1931.

[6] Whelan, J.I., J.M.R. Graham, and J. Peiro, A free-surface and blockage correction for tidal turbines. Journal of Fluid Mechanics, 2009. 624: p. 281-291.

[7] McAdam, R.A., et al., Experimental testing of the transverse horizontal axis water turbine. Renewable Power Generation, IET, 2010. 4(6): p. 510-518.

[8] Jacobs, E.N. and A. Sherman, Airfoil Section Characteristics as Affected by Variations of the Reynolds Number. NACA Report no. 586, 1937.

[9] Jacobs, E.N., K.E. Ward, and R.M. Pinkerton, The characteristics of 78 related airfoil sections from tests in the variable-density wind tunnel. NACA Report 460 1933.